HHS Public Access

Author manuscript

Science. Author manuscript; available in PMC 2015 March 04.

Published in final edited form as:

Science. 2014 June 6; 344(6188): 1178–1182. doi:10.1126/science.1253895.

Specific disruption of thalamic inputs to the auditory cortex in schizophrenia models

Sungkun Chun, **Joby J. Westmoreland**, **Ildar T. Bayazitov**, **Donnie Eddins**, **Amar K. Pani**, **Richard J. Smeyne**, **Jing Yu**, **Jay A. Blundon**, and **Stanislav S. Zakharenko***

Department of Developmental Neurobiology, St. Jude Children's Research Hospital, Memphis, TN 38105, USA

Abstract

Auditory hallucinations in schizophrenia are alleviated by antipsychotic agents that inhibit D2 dopamine receptors (Drd2s). The defective neural circuits and mechanisms of their sensitivity to antipsychotics are unknown. We identified a specific disruption of synaptic transmission at thalamocortical projections in the auditory cortex in murine models of schizophrenia-associated 22q11 deletion syndrome (22q11DS). This deficit is caused by an aberrant elevation of Drd2 in the thalamus, which renders 22q11DS thalamocortical projections sensitive to antipsychotics and causes a deficient acoustic startle response similar to that observed in schizophrenic patients. Haploinsufficiency of the microRNA-processing gene *Dgcr8* is responsible for the Drd2 elevation and hypersensitivity of auditory thalamocortical projections to antipsychotics. This suggests that Dgcr8-microRNA-Drd2–dependent thalamocortical disruption is a pathogenic event underlying schizophrenia-associated psychosis.

Schizophrenia (SCZ) is one of the most debilitating forms of mental illness (1). Positive symptoms of SCZ, including auditory hallucinations, are among the most enigmatic. Antipsychotic agents acting via D2 dopamine receptors (Drd2s) alleviate auditory hallucinations in most patients (2, 3), but do not treat other symptoms (cognitive deficits, dampened emotions, social withdrawal) (4). Sensory cortex malfunction has been implicated in hallucinations (5, 6), but which neural circuits become faulty and how they develop selective sensitivity to antipsychotics are unknown.

We tested synaptic transmission at excitatory projections in the auditory cortex (ACx) of *Df(16)1*/+ mice (7, 8), a mouse model of 22q11DS (9) (Fig. 1A). Because positive symptoms emerge during adolescence or early adulthood, we used mature (4- to 5-month-old) mice. We measured evoked AMPA receptor (AMPAR)–mediated excitatory postsynaptic currents (EPSCs) from layer (L) 3/4 pyramidal neurons, the main thalamorecipient neurons in ACx (10), in response to stimulation of thalamocortical (TC) or corticocortical (CC [L3/4-L3/4 or L1-L3/4]) projections in slices containing the auditory thalamus (the ventral medial geniculate nucleus [MGv]), ACx, and hippocampus (Fig. 1B–E). We also measured synaptic transmission at corticothalamic (CT) projections by recording CT EPSCs in MGv thalamic neurons (Fig. 1F) and at hippocampal CA3-CA1

*To whom correspondence should be addressed. stanislav.zakharenko@stjude.org.

projections by recording field excitatory postsynaptic potentials (fEPSPs) (Fig. 1G). Only TC projections were deficient in *Df(16)1/+* mice compared to wild-type (WT) littermates (30 [WT]/30 [*Df(16)1/+*] neurons) (Figs. 1C, S1), and this deficit occurred in both female and male mice (Fig. S2). Synaptic transmission at CC (19/19 and 17/16 neurons for L3/4-L3/4 and L1-L3/4, respectively), CT (14/16 neurons), or hippocampal (24/29 slices) projections was normal (Figs. 1D–G, S1).

Several findings supported that TC deficiency in *Df(16)1/+* mice is presynaptic. Two-photon calcium imaging in dendritic spines of L3/4 neurons loaded with the calcium indicator Fluo-5F and cytoplasmic dye Alexa 594 (Fig. 1H) identified functional TC inputs (Fig. 1I). The distribution of thalamic inputs on dendritic trees and the calcium-transient amplitudes were normal (Fig. 1J, K), but calcium-transient probability was deficient at TC synapses of *Df(16)1/+* mice (Fig. 1L). Paired-pulse depression evoked electrically or optogenetically was reduced at *Df(16)1/+* TC projections (Fig. S3). The FM 1–43 assay (11) showed slower dye release from TC terminals in mutant mice (Fig. S4). Monosynaptic TC N-methyl-D-aspartate receptor (NMDAR)–dependent EPSCs were also deficient in *Df(16)1/+* mice (Fig. S5). However, the NMDAR/AMPAR ratio was unaffected (Fig. S6). Minimal electrical stimulation of the thalamic radiation that typically evoked unitary EPSCs (successes) or no ESPCs (failures) revealed reduced release probability in TC projections of *Df(16)1/+* mice (Fig. S7). A synaptic deficiency rather than a decrease in excitability of thalamic neurons seemed to cause the presynaptic deficit at *Df(16)1/+* TC projections (Fig. S8).

Antipsychotics haloperidol (1 μM) and clozapine (40 μM) reversed the synaptic defect of *Df(16)1/+* TC connections (Figs. 2, S9). Normalized EPSC data revealed that *Df(16)1/+* (but not WT) TC projections are sensitive to antipsychotics (Figs. 2B, S9A). CC projections of both genotypes remained insensitive to the drugs (Figs. 2C, S9B, S10–12). Response of mutant TC projections to antipsychotics was dose-dependent (Fig. S13). Approximately 85% of mutant TC neurons responded more strongly than WT neurons to antipsychotics (Fig. S14). In contrast to ACx, TC projections in *Df(16)1/+* somatosensory or visual cortices were not sensitive to haloperidol (Fig. S15).

The sensitivity of *Df(16)1/+* TC projections to antipsychotics was mediated by Drd2s. The Drd2-specific antagonist L-741,626 (20 nM) enhanced TC EPSCs in *Df(16)1/+* but not WT mice (Fig. 2D). Subsequent application of haloperidol did not induce an additional effect, suggesting that both agents act through Drd2s (Fig. 2D). Drd2 agonist quinpirole (0.5–20 μM) did not affect TC or CC EPSCs in WT or *Df(16)1/+* mice (Fig. S16). Dopaminergic projections from the ventral tegmental area (VTA) were present in the thalamic radiation and ACx (Fig. S17) and, therefore, may deliver dopamine to TC projections. We hypothesized that ambient dopamine in the MGv and ACx may activate abnormally upregulated Drd2 in TC projections of *Df(16)1/+* mice. Quantitative real-time PCR (Fig. 2E) and in situ hybridization (Fig. 2F, S18) revealed an increase in *Drd2* transcript levels in *Df(16)1/+* MGv. Splice variants of *Drd2* (*D2Short* and *D2Long*) (Fig. S19) and Drd2 protein levels (Fig. 2G) were comparably increased in *Df(16)1/+* MGv. Transcript and protein levels increased in the thalamus but not the cortex, hippocampus, and striatum (Fig. 2E, G). However, total dopamine levels in all regions assayed were comparable between

both genotypes (Fig. S20). In postmortem human tissues (Fig. 2H, Table S1), DRD2 protein levels in the MGv were higher in SCZ patients than in healthy controls ($P < 0.001$, 13 patients/group).

We next screened 12 mouse strains carrying hemizygous deletions of gene clusters or individual genes within the microdeletion for haloperidol sensitivity (Fig. 3A). We measured TC EPSCs before and after haloperidol in mutants and WT littermates. In addition to *Df(16)1*/+, only *Df(16)2*/+ and *Dgcr8*$^{+/-}$ mice responded to haloperidol (Fig. 3B). The miRNA-processing gene *Dgcr8* is encoded within the *Df(16)2* region (Fig 3A). Like *Df(16)1*/+, approximately 80% of *Dgcr8*$^{+/-}$ neurons responded more strongly than WT neurons to the antipsychotics (Figs. S21, S22), implying an impaired flow of acoustic information in *Dgcr8*$^{+/-}$ mice. Acoustic startle response was lower in mature *Dgcr8*$^{+/-}$ mice than in WT littermates (22/25 mice, $P < 0.05$) (Fig. 3C). This deficit may affect prepulse inhibition (PPI) of acoustic startle, a characteristic feature of SCZ in animal models and patients. *Dgcr8*$^{+/-}$ mice were deficient in PPI (24/29 mice, $P < 0.05$ at 90 dB sound pressure level [SPL]) (Fig. 3D), and this deficit was rescued by haloperidol ($P < 0.05$ at 90 dB SPL) (Fig. 3D).

Consistent with the notion that *Dgcr8* haploinsufficiency underlies the sensitivity of TC projections to antipsychotics in 22q11DS, *Drd2* mRNA levels were found to be increased in the MGv but not cortex of *Dgcr8*$^{+/-}$ mice (Fig. 3E). *Znf74l-Ctp*/+ and *Df(16)5*/+ microdeletions, which do not include *Dgcr8*, produced no increase in *Drd2* (Fig. 3E), but *Df(16)2*/+ mice carrying a *Dgcr8*-containing microdeletion did (Fig. S23).

Conditional *Dgcr8* hemizygous deletion in MGv neurons (Fig. 3F) rendered TC projections sensitive to antipsychotics (Fig. 3G), indicating that MGv-specific reduction in *Dgcr8* underlies TC deficiency in 22q11DS mice.

To test whether Drd2 elevation causes TC deficiency, we knocked down *Drd2* in MGv neurons (Fig. 4A, S24A). *Drd2* siRNA but not scrambled (control) siRNA decreased *Drd2* levels in MGv (Fig. S24B) and eliminated the sensitivity of mutant TC projections to antipsychotics (Fig. 4A,B). Drd2 overexpression in MGv excitatory neurons (Fig. 4C) made WT TC projections sensitive to haloperidol (Fig. 4D) and caused deficits in acoustic startle and PPI in WT mice (Fig. 4E, F).

Thus, we have identified an SCZ-associated microdeletion that upregulates Drd2 in thalamic neurons, disrupts synaptic transmission at TC projections to the ACx, and is caused by haploinsufficiency of *Dgcr8*. This mechanism integrates several competing SCZ models [e.g., dopamine hyperfunction theory (2), glutamatergic hypofunction theory (12), TC disconnectivity theory (13), and TC loop dysfunction models (14)]. Our results indicate disturbances in the Dgcr8-miRNA-Drd2 pathway in thalamic projections to the ACx as a pathogenic mechanism that alters the normal flow of auditory information and thereby contributes to positive symptoms of SCZ.

Supplementary Material

Refer to Web version on PubMed Central for supplementary material.

Acknowledgments

This work was supported, in part, by National Institute of Health grants R01 MH097742, R01 MH095810, and R01 DC012833 and the American Lebanese Syrian Association Charities (ALSAC). We thank Elizabeth Illingworth, Peter Scambler, Anthony Wynshaw-Boris, Joseph Gogos, Stephen Strittmatter, Bernice Morrow, and Elain Fuchs for providing mutant mice; Andree Lessard and the Maryland Brain Collection for providing postmortem human brain samples; Kenneth J. Sample and Prakash Devaraju for technical assistance; and St. Jude, University of Tennessee, University of North Carolina, and University of Pennsylvania Vector Cores for producing AAVs and lentiviruses.

References and notes

1. Insel TR. Rethinking schizophrenia. Nature. 2010; 468:187–193. [PubMed: 21068826]
2. Carlsson A. The current status of the dopamine hypothesis of schizophrenia. Neuropsychopharmacology. 1988; 1:179–186. [PubMed: 3075131]
3. Snyder SH. Drugs for a new millennium. Philos. Trans. R. Soc. Lond B Biol. Sci. 1999; 354:1985–1994. [PubMed: 10670019]
4. Miyamoto S, Miyake N, Jarskog LF, Fleischhacker WW, Lieberman JA. Pharmacological treatment of schizophrenia: a critical review of the pharmacology and clinical effects of current and future therapeutic agents. Mol. Psychiatry. 2012; 17:1206–1227. [PubMed: 22584864]
5. Dierks T, et al. Activation of Heschl's gyrus during auditory hallucinations. Neuron. 1999; 22:615–621. [PubMed: 10197540]
6. Hubl D, Koenig T, Strik WK, Garcia LM, Dierks T. Competition for neuronal resources: how hallucinations make themselves heard. Br. J Psychiatry. 2007; 190:57–62. [PubMed: 17197657]
7. Lindsay EA, et al. Congenital heart disease in mice deficient for the DiGeorge syndrome region. Nature. 1999; 401:379–383. [PubMed: 10517636]
8. Lindsay EA, et al. Tbx1 haploinsufficieny in the DiGeorge syndrome region causes aortic arch defects in mice. Nature. 2001; 410:97–101. [PubMed: 11242049]
9. The 22q11DS is caused by the hemizygous deletion of a 1.5- to 3-megabase region of the q arm of human chromosome 22, and SCZ develops in approximately 30% of patients with 22q11DS. *Df(16)1/+* mice carry a hemizygous deletion of 23 genes in the syntenic region of chromosome 16.
10. Smith PH, Populin LC. Fundamental differences between the thalamocortical recipient layers of the cat auditory and visual cortices. J Comp Neurol. 2001; 436:508–519. [PubMed: 11447593]
11. Zakharenko SS, Zablow L, Siegelbaum SA. Visualization of changes in presynaptic function during long-term synaptic plasticity. Nat. Neurosci. 2001; 4:711–717. [PubMed: 11426227]
12. Coyle JT. The glutamatergic dysfunction hypothesis for schizophrenia. Harv. Rev. Psychiatry. 1996; 3:241–253. [PubMed: 9384954]
13. Woodward ND, Karbasforoushan H, Heckers S. Thalamocortical dysconnectivity in schizophrenia. Am. J Psychiatry. 2012; 169:1092–1099. [PubMed: 23032387]
14. Behrendt RP. Hallucinations: synchronisation of thalamocortical gamma oscillations underconstrained by sensory input. Conscious. Cogn. 2003; 12:413–451. [PubMed: 12941286]
15. Cruikshank SJ, Rose HJ, Metherate R. Auditory thalamocortical synaptic transmission in vitro. J. Neurophysiol. 2002; 87:361–384. [PubMed: 11784756]
16. Blundon JA, Bayazitov IT, Zakharenko SS. Presynaptic gating of postsynaptically expressed plasticity at mature thalamocortical synapses. J. Neurosci. 2011; 31:16012–16025. [PubMed: 22049443]
17. Bolshakov VY, Siegelbaum SA. Regulation of hippocampal transmitter release during development and long-term potentiation. Science. 1995; 269:1730–1734. [PubMed: 7569903]
18. Richardson RJ, Blundon JA, Bayazitov IT, Zakharenko SS. Connectivity patterns revealed by mapping of active inputs on dendrites of thalamorecipient neurons in the auditory cortex. J Neurosci. 2009; 29:6406–6417. [PubMed: 19458212]
19. Chun S, Bayazitov IT, Blundon JA, Zakharenko SS. Thalamocortical long-term potentiation becomes gated after the early critical period in the auditory cortex. J Neurosci. 2013; 33:7345–7357. [PubMed: 23616541]

20. Boyden ES, Zhang F, Bamberg E, Nagel G, Deisseroth K. Millisecond-timescale, genetically targeted optical control of neural activity. Nat. Neurosci. 2005; 8:1263–1268. [PubMed: 16116447]

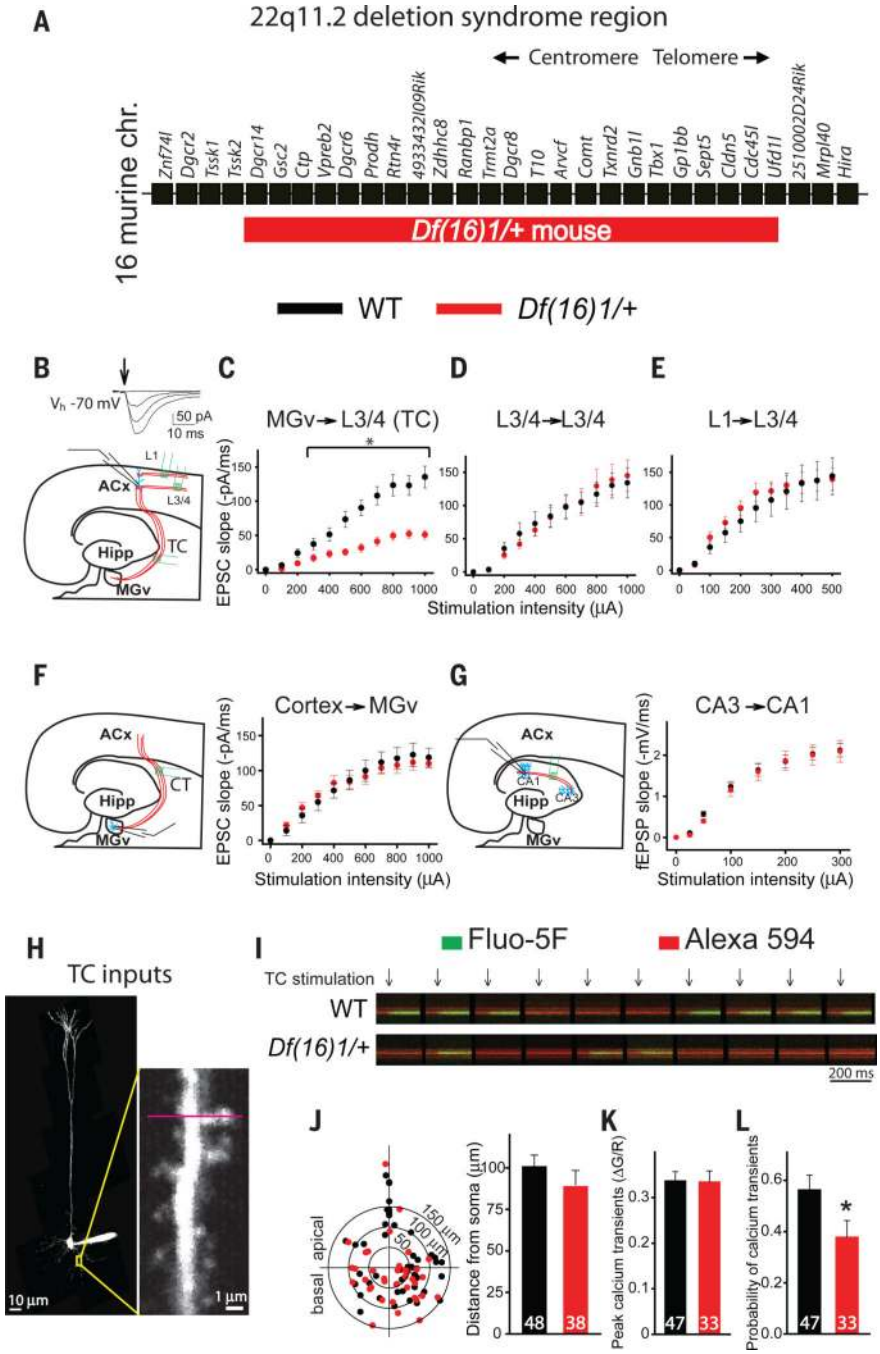

Fig. 1. Specific deficit of TC synaptic transmission to the ACx of 22q11DS mice

(**A**) Map of 22q11DS orthologs in *Df(16)1/+* mice. (**B**) Voltage-clamp recordings in thalamorecipient L3/4 pyramidal neurons. Arrow: electrical stimulation (**top**). TC slices containing MGv, hippocampus (Hipp), and ACx (**bottom**). (**C–E**) Input–output relationships between stimulation intensity and EPSCs at TC (MGv-L3/4) (**C**), L3/4-L3/4 (**D**), and L1-L3/4 (**E**) projections. (**F, G**) CT EPSC and CA3-CA1 fEPSP recordings (**left**) and input–output relationship (**right**). (**H**) L3/4 pyramidal neuron filled with Fluo-5F and Alexa 594 (**left**) to visualize dendritic spines (**right**). Red line represents the line scan. (**I**)

Calcium transients in a dendritic spine in response to a single TC stimulation (arrows) repeated 10 times (0.1 Hz). (**J**) TC input location on dendritic trees of L3/4 pyramidal neurons (48 [WT]/38 [*Df(16)1*/+] spines from 17 [WT]/11 [*Df(16)1*/+] neurons) (**left**); (0;0), soma coordinates. Average distances from soma to TC inputs (**right**). (**K**, **L**) Calcium transient amplitudes (**K**) and probabilities (**L**) in response to 10 single TC stimulations. Numbers of spines tested are shown inside columns. **P* < 0.05 (C, L).

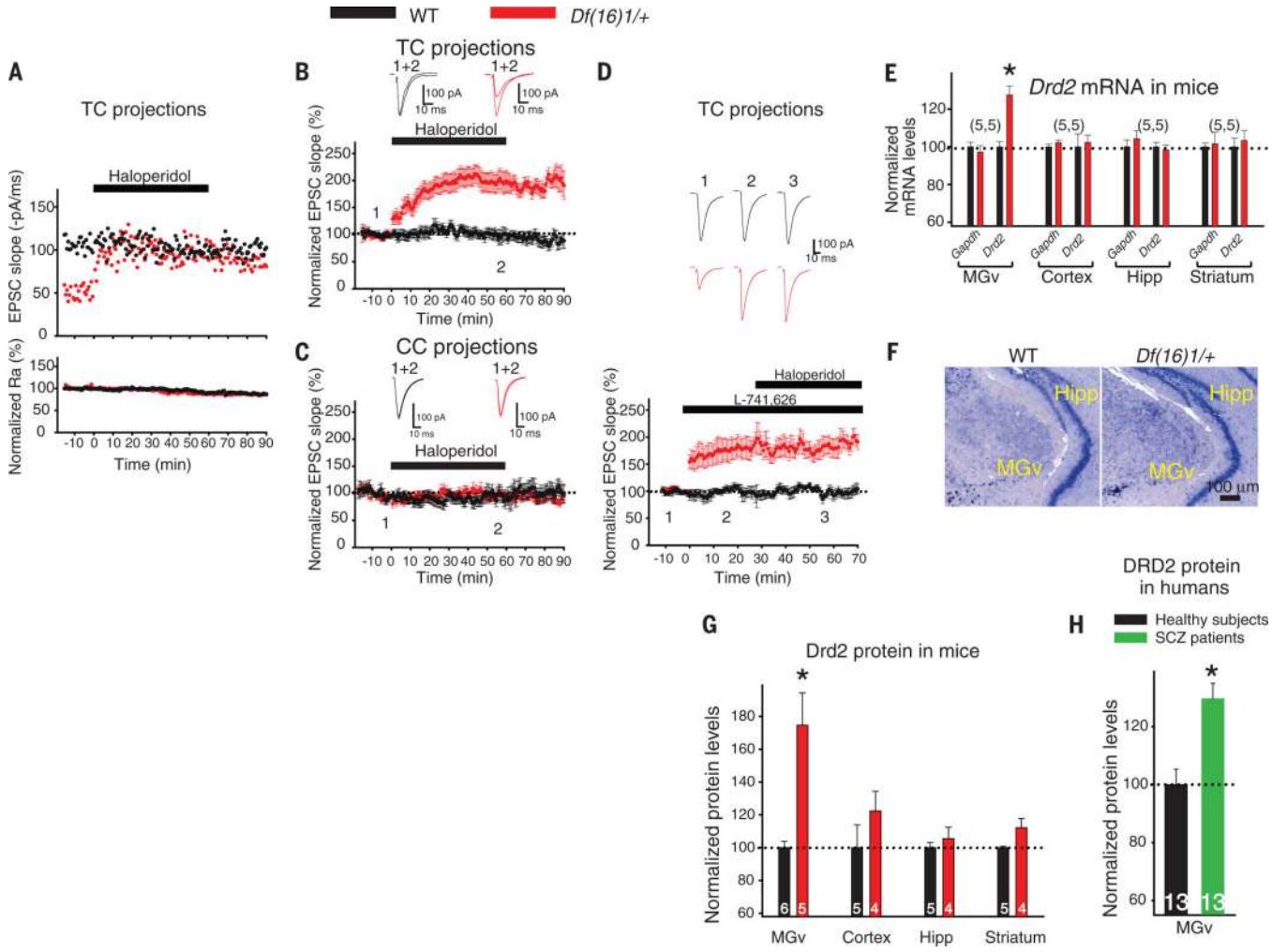

Fig. 2. The 22q11DS microdeletion renders TC projections abnormally sensitive to antipsychotics due to increased Drd2s in the MGv

(**A**) TC EPSCs (**top**) and access resistance (Ra) (**bottom**) during repeated TC stimulations (0.05 Hz, 600 μA) before and after haloperidol (1 μM). (**B, C**) Mean EPSCs normalized to initial baseline at TC ($P < 0.001$, 16/21 neurons) (**B**) and L3/4-L3/4 CC projections ($P = 0.75$, 15/14 neurons) (**C**) before and after haloperidol. (**D**) Normalized TC EPSCs before and after L-741,626 (20 nM) and haloperidol (5/12 neurons). Insets: representative EPSC traces. (**E**) Average mRNA levels of *Drd2* normalized to *Gapdh* in different brain regions. (**F**) *Drd2* in situ hybridization. (**G, H**) Average Drd2 and DRD2 protein levels normalized to β-actin in mice (**G**) and MGv from postmortem tissues of healthy human controls and patients with SCZ (**H**). Numbers of mice or human samples are shown inside columns or parentheses. *$P < 0.05$ (E, G, H).

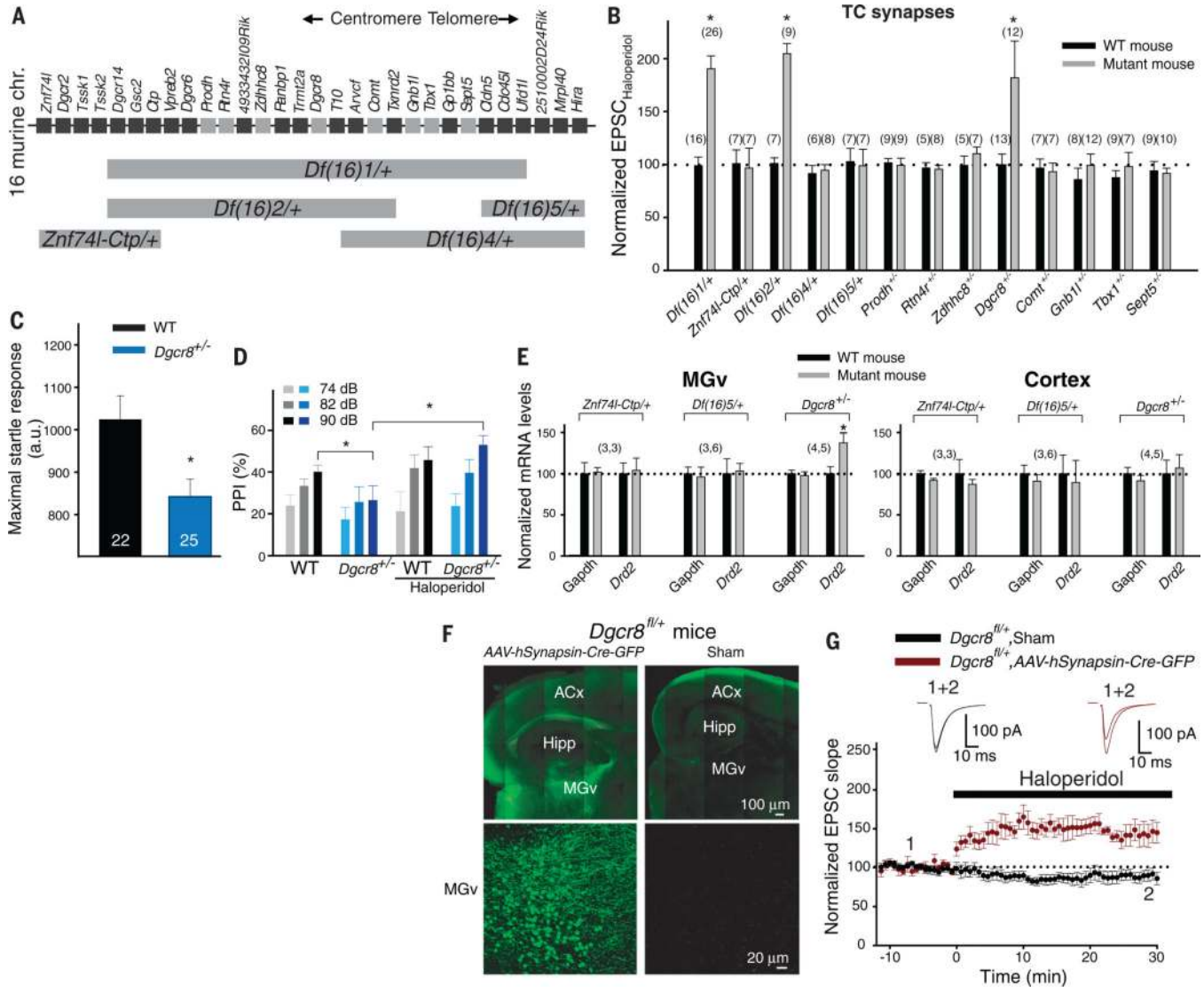

Fig. 3. *Dgcr8* haploinsufficiency causes abnormal TC sensitivity to antipsychotics and acoustic startle deficit in 22q11DS mice

(**A**) Mouse strains carrying hemizygous multigene or single-gene deletions within the 22q11DS region. Light gray boxes: mouse strains used. (**B**) Average haloperidol effect on TC EPSCs ($EPSC_{haloperidol}$) in 13 mutant mouse lines and WT littermates normalized to baseline (before haloperidol). EPSC slopes were measured 30 min after drug application. Baselines were established by adjusting stimulation intensities to elicit peak EPSC amplitudes of 100–200 pA. (**C**) Average maximal acoustic startle response at 120 dB SPL. (**D**) Mean PPI of acoustic startle before and after haloperidol. (**E**) Mean *Drd2* mRNA levels (normalized to *Gapdh*) in MGv (**left**) and cortex (**right**). (**F**) Low- (**top**) and high-magnification (**bottom**) images of TC slice from $Dgcr8^{fl/+}$ mice injected with *AAV-hSynapsin-Cre-GFP* (**left**) or ACSF (Sham, **right**). (**G**) Mean TC EPSCs before and after haloperidol in $Dgcr8^{fl/+}$ mice injected in vivo with *AAV-hSynapsin-Cre-GFP* or sham ($P < 0.05$, 8/6 neurons). Insets show representative TC EPSCs. Dotted line: baseline. Numbers of neurons (B) or mice (C, E) shown inside columns or parentheses.*$P < 0.05$.

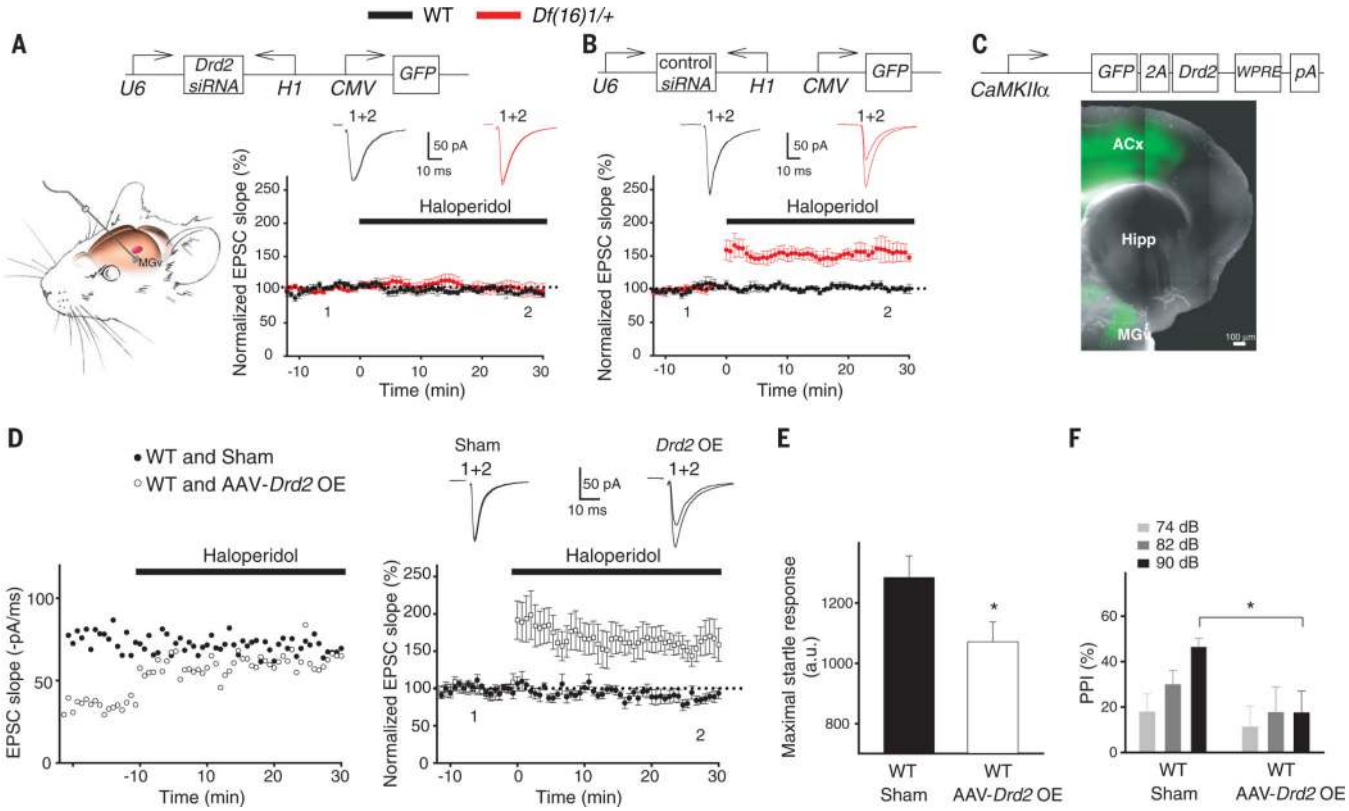

Fig. 4. Aberrant Drd2 elevation in MGv neurons is necessary and sufficient to render TC projections sensitive to antipsychotics

(**A, B**) *Drd2* (**A, top**) and control (**B, top**) siRNA viruses. In vivo MGv viral injection (**A, bottom, left**). Mean TC EPSCs before and after haloperidol in mice injected with *Drd2* siRNA (**A, bottom, right**) ($P = 0.67$, 9/11 neurons) or control siRNA viruses (**B, bottom**) ($P = 0.016$, 7/9 neurons). (**C**) Composition of the *Drd2-OE* virus (woodchuck hepatitis posttranscriptional regulatory element [*WPRE*], polyA signal [*pA*]) (**top**) and TC slice showing GFP in MGv neurons (**bottom**). (**D**) Representative TC EPSCs (**left**) and mean normalized TC EPSCs (**right**) before and after haloperidol from WT mice injected with *Drd2-OE* or sham ($P < 0.05$, 7/9 neurons). (**E, F**) Acoustic startle response (**E**) at 120 dB SPL and PPI (**F**) in WT mice injected with *Drd2-OE* or sham (10 mice each) into MGv, $*P < 0.05$. Dotted lines: baseline; insets: representative TC EPSCs.